

Supplementary material

S1. Analysis of the rise time in YC3.60 time-resolved fluorescence data

To check whether it is possible to resolve two components in the time-dependent rise of acceptor fluorescence intensity, several simulations were performed, namely for YC3.60 in the presence of Ca^{2+} where the FRET efficiency is about 95% and for YC3.60 in the absence of Ca^{2+} where the FRET efficiency is about 50%. The rise times for the simulations were calculated from the lifetimes of ECFP in case of 95% FRET efficiency ($\alpha_1 = 0.3$, $\tau_1 = 50 \text{ ps}$, $\alpha_2 = 0.7$, $\tau_2 = 180 \text{ ps}$) and of 50 % FRET efficiency ($\alpha_1 = 0.3$, $\tau_1 = 500 \text{ ps}$, $\alpha_2 = 0.7$, $\tau_2 = 1800 \text{ ps}$). In other simulations 3% or 20% of donor crosstalk (2.7 ns) in the acceptor detection window was allowed. The model used for the simulations was:

$$I = [A\{N_{pos}e^{-\frac{t}{\tau_A}} - N_{neg}\left(\sum_i \alpha_i e^{-\frac{t}{\tau_{ni}}}\right)\} + Be^{-\frac{t}{\tau_D}}] \otimes Irf$$

where τ_A is the fluorescence lifetime of the acceptor, τ_D is the fluorescence lifetime of the unquenched donor, τ_{ni} are fluorescence rise times and α_i their relative amplitudes ($\sum \alpha_i = 1$), N_{pos}

and N_{neg} are scaling factors, B is the amplitude that accounts for crosstalk of unquenched donor fluorescence, such that $A+B=1$, Irf is the instrumental response function and \otimes is the convolution operator. The measured fluorescence decay of xanthione in ethanol with a fluorescence lifetime of 14 ps was used in the reference convolution method. A time scale of 1 ps/ch and 4000 data channels were used and Poissonian noise was added to the theoretical decay equivalent to a signal to noise ratio of experimentally observed fluorescence decay with approximately 2000 photons in the maximum of the curve.

Theoretical fluorescence traces of donor-excited YC3.60 in the acceptor detection window are presented in Fig. S1-1. It is immediately clear that the effect of spectral crosstalk ($B=0.03$ or $B=0.20$) is larger in case of slower rise times, since the curves are clearly separated.

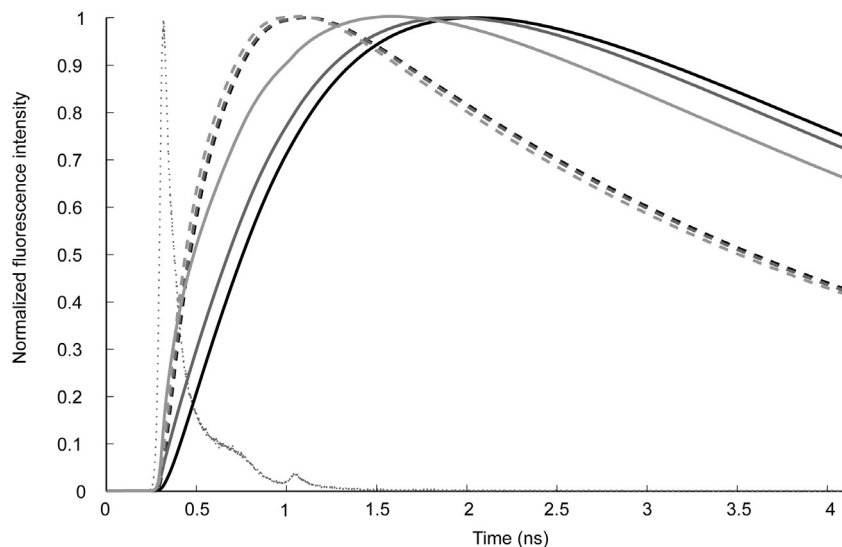


Figure S1-1. Theoretical fluorescence traces of donor-excited YC3.60 in the acceptor detection window. Dashed lines represent data with a FRET efficiency of 95%, while solid lines represent data with a FRET efficiency of 50%. Black lines represent data without spectral crosstalk and grey lines (from dark grey to light grey) are data with respectively 3% and 20% of crosstalk. The IRF (dotted line) is also presented.

The results of the analysis of simulated data without crosstalk are presented in Table S1-1 and in Fig. S1-2.

Table S1-1. Parameters used during simulation and parameter estimates after single and double component analysis without crosstalk

Input parameters for simulation					Single rise-time analysis			Double rise-time analysis					
α_J %	τ_{n1} (ps)	τ_{n2} (ps)	$\langle\tau_n\rangle$ (ps)	τ (ps)	τ_n (ps)	τ (ps)	χ^2	α_J %	τ_{n1} (ps)	τ_{n2} (ps)	$\langle\tau_n\rangle$ (ps)	τ (ps)	χ^2
30	50	180	141	3100	145	3100	1.09	30	62	181	145	3100	1.03
30	500	1800	1410	3100	897	3100	1.82	28	470	1600	1283	3100	1.01

The first entry corresponds to parameters for YC3.60 in the presence of calcium. The second entry corresponds to those for YC3.60 in the absence of calcium.

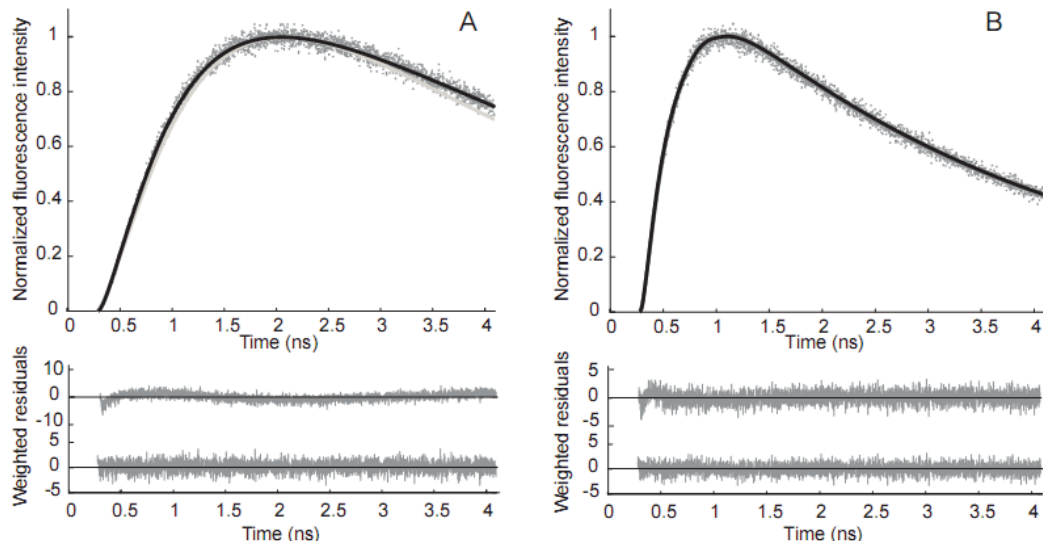


Figure S1-2. The results of the analysis of simulated data with donor excitation and acceptor detection without crosstalk. A: Simulated and fitted fluorescence decay of YC3.60 in the absence of Ca^{2+} ; B: Simulated and fitted fluorescence decay of YC3.60 in the presence of Ca^{2+} , weighted residuals from a single-component analysis are shown in the upper panel and weighted residuals from a double-component analysis are shown in the lower panel.

In case of 50% FRET efficiency (Fig. S1-2A) the recovered rise times (470 ps and 1600 ps) are close to the values used for the simulation (500 ps and 1800 ps) leading to an average lifetime of 1283 ps close to the expected one of 1410 ps (see Table S1-1). The recovered values strongly depend on the estimated decay time of the acceptor. Analysis in this case should be done with a fixed fluorescence lifetime of the acceptor. In case of single-component rise time analysis it is observed that the average lifetime is even shorter (897 ps) (see Table S1-1). In addition, the fit quality is worse than for a fit with two rise times (see χ^2 value in Table S1-1 and residuals in Fig. S1-2A).

In case of 95% FRET efficiency (Fig. S1-2B) the two fast components (50 ps and 180 ps) are not completely recovered from the rising part of the acceptor fluorescence decay curve (62 ps and 181 ps, see Table S1-1). The reason might be due to the finite width of the instrumental response function (~ 30 ps) and distortions induced by convolution. Analysis using the single-component model yields a rise time of 145 ps, which is very close to the average rise time of 141 ps (see Table S1-1). The quality of the fit is similar for both single- and double-component analysis.

The effect of crosstalk in the analysis of simulated data has been presented in Table S1-2. By comparing the recovered time constants with those in the absence crosstalk (Table S1-1) it can be concluded that the optimized rise times remain similar with a slight tendency for the longer

average rise time to slightly increase with increasing percentage of crosstalk (from 1283 ps (0%), 1330 ps (3%) to 1670 ps (20%)).

Table S1-2. Parameters used during simulation and parameter estimates after single and double component analysis with 3% and 20% of crosstalk.

3% of crosstalk

Input parameters for simulation					Single rise-time analysis			Double rise-time analysis					
α_I %	τ_{n1} (ps)	τ_{n2} (ps)	$\langle\tau_n\rangle$ (ps)	τ (ps)	τ_n (ps)	τ (ps)	χ^2	α_I %	τ_{n1} (ps)	τ_{n2} (ps)	$\langle\tau_n\rangle$ (ps)	τ (ps)	χ^2
30	50	180	141	3100	144	3100	1.05	29	53	176	140	3100	0.99
30	500	1800	1410	3100	912	3100	1.54	29	486	1675	1330	3100	0.99

20% of crosstalk

Input parameters for simulation					Single rise-time analysis			Double rise-time analysis					
α_I %	τ_{n1} (ps)	τ_{n2} (ps)	$\langle\tau_n\rangle$ (ps)	τ (ps)	τ_n (ps)	τ (ps)	χ^2	α_I %	τ_{n1} (ps)	τ_{n2} (ps)	$\langle\tau_n\rangle$ (ps)	τ (ps)	χ^2
30	50	180	141	3100	133	3100	1.03	18	43	147	128	3100	1.03
30	500	1800	1410	3100	969	3100	1.31	26	500	2082	1670	3100	1.03

An important conclusion is that a double-component intensity rise analysis clearly recovers the average donor fluorescence lifetime in the presence of acceptor $\langle\tau_{DA}\rangle$, which can then be used for calculation of the FRET efficiency from $E = 1 - \langle\tau_{DA}\rangle/\langle\tau_D\rangle$. Short, average rise times are already recovered after a single-component analysis. The simulations showed that it is better to fix the long decay time in the analysis.

A considerable simplification is introduced, when there is only one donor fluorescence lifetime present.

S2. The orientation factor κ^2 in FRET

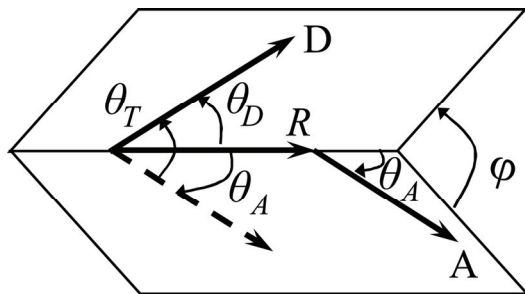


Figure S2-1. Dependence of the orientation factor κ^2 on the direction of transition dipole moments of donor and acceptor.

The orientation factor κ^2 for a donor-acceptor pair depends on three orientation angles: the angle (θ_D) between the emission transition dipole moment of the donor (μ_D) and the line connecting the centres of the donor and acceptor chromophores, the separation vector R , the angle (θ_A) between the absorption transition dipole moment of the acceptor (μ_A) and the separation vector and the angle (θ_T) between transition dipole moments μ_D and μ_A (Fig. S2-1). Two planes are formed by μ_D and R and by μ_A and R , intersecting at R and under an angle φ . The ‘experimental’ angle θ is equivalent to θ_T . The orientation factor can be expressed in two ways in terms of the various angles:

$$\kappa^2 = (\cos\theta_T - 3\cos\theta_D \cos\theta_A)^2$$

$$\kappa^2 = (\sin\theta_D \sin\theta_A \cos\varphi - 2\cos\theta_D \cos\theta_A)^2.$$

One can make 3D plots of κ^2 (z-axis) *versus* θ_D (y-axis) and *versus* θ_A (x-axis) for certain values of θ_T and estimate lower and upper values of possible κ^2 values. These graphs are presented in Fig. S3 for both $\theta_T = 46^\circ$ and $\theta_T = 62^\circ$.

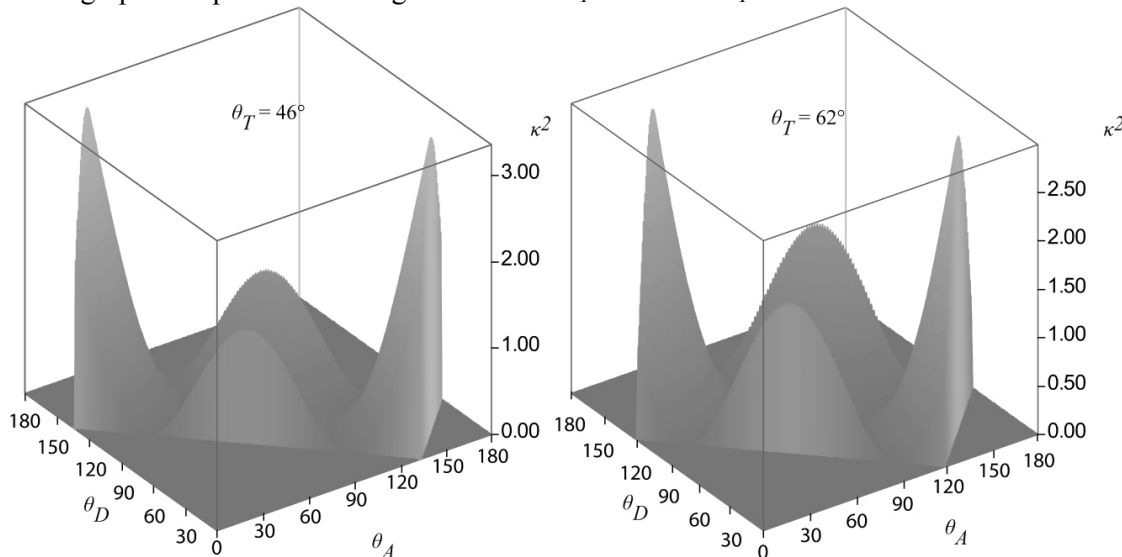


Figure S2-2. Graphical presentations of κ^2 *versus* θ_D and θ_A for $\theta_T = 46^\circ$ and $\theta_T = 62^\circ$.

From both graphs it can be noticed that the maximum value of κ^2 is between 2.5 ($\theta_T = 62^\circ$) and 3 ($\theta_T = 46^\circ$).

The critical transfer distance R_0 is plotted against κ^2 for the ECFP-Venus couple in Fig. S2-3. When κ^2 changes from 0.5 to 2.5 the change in R_0 is from 4.5 nm to 5.9 nm, illustrating that a 5-fold increase of orientation factor brings about a 1.3-fold increase of critical distance. A very low value of $\kappa^2 = 0.1$ already yields a $R_0 = 3.2$ nm.

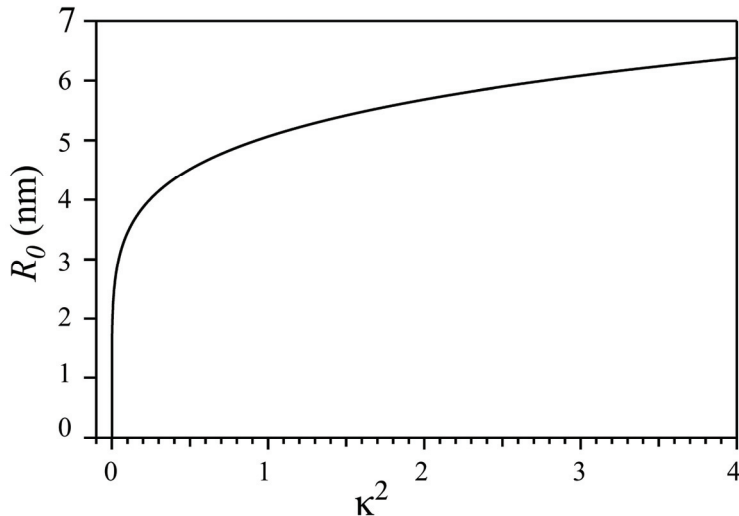


Figure S2-3. The dependence of the critical distance R_0 on the orientation factor κ^2 in case of FRET between ECFP and Venus. The quantum yield of the donor is 0.39, the refractive index of the medium is assumed to be 1.33 and the spectral overlap integral is $1.55 \times 10^{15} \text{ nm}^4 \text{ M}^{-1} \text{ cm}^{-1}$.